Journal of proteome research

pubs.acs.org/jpr

Article

Deep Time Course Proteomics of SARS-CoV- and SARS-CoV-2-Infected Human Lung Epithelial Cells (Calu-3) Reveals Strong Induction of Interferon-Stimulated Gene Expression by SARS-CoV-2 in Contrast to SARS-CoV

Marica Grossegesse, Daniel Bourquain, Markus Neumann, Lars Schaade, Jessica Schulze, Christin Mache, Thorsten Wolff, Andreas Nitsche, and Joerg Doellinger*

Cite This: https://doi.org/10.1021/acs.jproteome.1c00783

Read Online

ACCESS | Metrics & More | Article Recommendations | Supporting Information

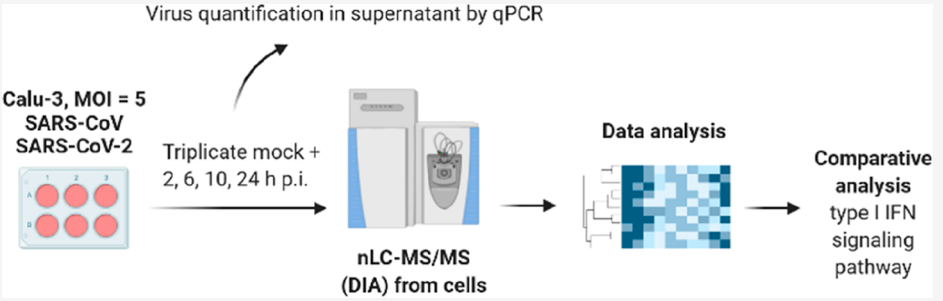

ABSTRACT: Severe acute respiratory syndrome (SARS)-CoV and SARS-CoV-2 infections are characterized by remarkable differences, including infectivity and case fatality rate. The underlying mechanisms are not well understood, illustrating major knowledge gaps of coronavirus biology. In this study, protein expression of the SARS-CoV- and SARS-CoV-2-infected human lung epithelial cell line Calu-3 was analyzed using data-independent acquisition−mass spectrometry. This resulted in a comprehensive map of infection-related proteome-wide expression changes in human cells covering the quantification of 7478 proteins across four time points. Most notably, the activation of interferon type-I response was observed, which is surprisingly absent in several proteome studies. The data reveal that SARS-CoV-2 triggers interferon-stimulated gene expression much stronger than SARS-CoV, which reflects the already described differences in interferon sensitivity. Potentially, this may be caused by the enhanced abundance of the viral M protein of SARS-CoV in comparison to SARS-CoV-2, which is a known inhibitor of type I interferon expression. This study expands the knowledge on the host response to SARS-CoV-2 infections on a global scale using an infection model, which seems to be well suited to analyze the innate immunity.

KEYWORDS: *SARS-CoV-2, coronavirus, interferon response, interferon-stimulated gene, proteomics, data-independent acquisition*

INTRODUCTION

In late 2019, the first cases of severe pneumonia of unknown origin were reported in Wuhan, China. Shortly afterward, a new coronavirus was discovered as the causative agent and named severe acute respiratory syndrome (SARS)-CoV-2 and the related disease COVID-19. The virus turned out to be highly infectious and caused a world-wide pandemic, which is still ongoing and has led to the death of >4,500,000 humans worldwide by September 2021. Already in 2002, another coronavirus, SARS-CoV, was discovered in China which caused an outbreak with about 780 deaths.[1] However, at this time, the outbreak could be controlled probably due to the lower infectivity of SARS-CoV compared to SARS-CoV-2.[2] SARS-CoV and SARS-CoV-2 share about 80% of their genome sequence and protein homology ranges between 40 and 94%.[3,4] Although both viruses mainly lead to respiratory tract infections and can cause severe pneumonia, they are characterized by remarkable differences, including infectivity and case fatality rate.[5] As the respiratory tract is the first and main target of SARS-CoV and SARS-CoV-2 infections, it seems conclusive to use airway epithelia cells to study the differences between these two viruses. However, no comparative proteomics study has been published using Calu-3 cells, which is the only permissive lung cell line available for SARS-CoV and SARS-CoV-2.[6] Other human lung cell lines, such as A549, are only susceptible to

Received: September 28, 2021

SARS-CoV-2 infection upon overexpression of the SARS-CoV receptor ACE2,[6] which was recently found to be an interferon-stimulated gene (ISG).[7] In the present study, we used data-independent acquisition−mass spectrometry (DIA−MS) to analyze the protein expression in Calu-3 cells infected with SARS-CoV and SARS-CoV-2 over the time course of 24 h. In total, 8391 proteins were identified, 7478 of which could be reliably quantified across the experiment. This results in a deep and comprehensive proteome map, which reflects time-dependent protein expression changes during SARS-CoV and SARS-CoV-2 infections and provides deep insights into the virus-specific immunomodulation of human lung cells.

METHODS

Cell Culture and Infection for Proteomics Experiments

Calu-3 cells (ATCC HTB-55) were cultivated in Eagle's minimum essential medium containing 10% fetal calf serum (FCS), 2 mM L-glutamine, and non-essential amino acids. A total of 5×10^5 cells per well were seeded in six-well plates and incubated overnight at 37 °C and 5% CO_2 in a humified atmosphere. The medium was removed, and the cells were infected with SARS-CoV (strain Hong Kong) or SARS-CoV-2 (hCoV-19/Italy/INMI1-isl/2020 (National Institute for Infectious Diseases, Rome, Italy, GISAID Accession EPI_ISL_410545) at a multiplicity of infection (MOI) of 5. Mock samples were treated with medium only. One hour post infection (p.i.), the cells were washed with phosphate-buffered saline (PBS), and fresh medium was added. After 2, 6, 8, 10, and 24 h p.i., the medium was removed and stored at −80 °C. The cells were washed with PBS and prepared for proteomics as described below. For each time point and virus, triplicate samples were taken. Additionally, triplicate mock samples per time point were taken.

Cell Culture and Infection for Verification Experiments

Calu-3 cells were propagated in DMEM containing 15% FCS, 2 mM L-glutamine, 100 U/ml penicillin, 100 μg/ml streptomycin, 1× non-essential amino acids, and 1 mM sodium pyruvate and incubated at 37 °C with 5% CO_2 in a humidified atmosphere. For differentiation, the cells were seeded in ThinCert tissue culture inserts (0.4 μm pore size) and were cultivated under an air−liquid-Interface (ALI) for 14 days prior to infection.

The cells were infected with SARS-CoV-2 [hCoV-19/Germany/BY-ChVir-929/2020, lineage B.1.153 (GISAID accession: EPI_ISL_406862)] or SARS-CoV (Frankfurt-1) at an MOI of 0.1 in D-PBS containing 0.3% BSA for 1 h at 37 °C. Afterward, the cells were washed apically with D-PBS, and fresh medium was added to the apical and basolateral chambers. To quantify the infectious virus particles, apical and basolateral supernatants were harvested at indicated time points and titrated on Vero E6 cells by the standard plaque titration assay.

Polymerase Chain Reaction

The amount of SARS-CoV and SARS-CoV-2 RNA in the supernatant was analyzed by qPCR at 2, 6, 8, 10, and 24 h p.i. Supernatants were extracted using the QIAamp Viral RNA Mini Kit (Qiagen, Hilden, Germany) according to manufacturer's recommendations and eluted in 60 μL of RNase-free water. Real-time polymerase chain reaction (PCR) targeting the viral E gene was carried out as described by Michel et al.[8] using the primers and probe used in the study published by Corman et al.[9] Quantification of viral genome equivalents was done using the SARS-CoV-2 E gene WHO reference PCR standard.

Enzyme-Linked Immunosorbent Assay

Supernatants of infected polarized Calu-3 cells were analyzed using the R&D DuoSet ELISA Kits for human IFNα (DY9345-05), IFNβ (DY814-05), IFNλ (DY1598B), IP-10 (DY266), and IL-6 (DY206) according to the manufacturer's instructions.

Immunoblotting

Calu-3 cell monolayers were washed once with prechilled PBS and lysed in 100 μL of ice cold lysis buffer (10 mM Tris/HCl, pH 7.5, 150 mM NaCl, 0.5 mM EDTA, and 1% NP40). After at least 30 min of incubation on ice, cell lysates were centrifuged at 15,000*g* and 4 °C for 10 min. The supernatants were supplemented with 20 μL of 6× Laemmli sample buffer containing 5% β-mercaptoethanol and boiled for 10 min. Afterward, protein samples were separated using reducing sodium dodecyl sulfate−polyacrylamide gel electrophoresis under denaturing conditions and transferred onto nitrocellulose membranes. The membranes were incubated with antibodies detecting the SARS-CoV-2 Spike protein (Genetex, GTX632604), human Stat 1 (Santa Cruz Biotechnology, Inc., sc-464), human IFIT 2 (Abcam, ab113112), or human GAPDH (Cell Signaling Technology, Inc., #2118), respectively. Incubation with a suitable secondary horseradish-peroxidase-conjugated antibody (Agilent Technologies Inc., P0260/P0217) allows development on X-ray films using the Super-Signal™ West Dura Extended Duration Substrate (Thermo Fischer Scientific).

IRF-Activity Reporter Assay

ACE2-A549-Dual cells were seeded into 96-well plates at 4×10^4 cells per well and incubated overnight at 37 °C and 5% CO_2 in a humified atmosphere. The cells were infected with either SARS-CoV or SARS-CoV-2 at an MOI of 1.0. At 2 days p.i., the interferon regulatory factor (IRF)-activity was assayed using the QUANTI-Luc luminescence reagent (InvivoGen, San Diego, CA, USA) and an INFINITE 200 PRO microplate reader (Tecan, Männedorf, Switzerland).

Sample Preparation for Proteomics

Samples were prepared for proteomics using sample preparation by easy extraction and digestion.[10] At first, the medium was removed and the cells were washed using PBS. Afterward, 200 μL of trifluoroacetic acid (TFA) (Thermo Fisher Scientific, Waltham, MA, USA) was added, and the cells were incubated at room temperature for 3 min. The samples were neutralized by transferring TFA to prepared reaction tubes containing 1.4 mL of 2 M TrisBase. After adding tris(2-carboxyethyl)phosphine to a final concentration of 10 mM and 2-chloroacetamide to a final concentration of 40 mM, the samples were incubated at 95 °C for 5 min. 200 μL of the resulting solutions was diluted 1:5 with water and subsequently digested for 20 h at 37 °C using 1 μg of Trypsin Gold, MS Grade (Promega, Fitchburg, WI, USA). The resulting peptides were desalted using 200 μL StageTips packed with three Empore SPE Disks C18 (3 M Purification Inc., Lexington, USA) and concentrated using a vacuum concentrator.[11,12] Dried peptides were suspended in 20 μL of 0.1% TFA and quantified by measuring the absorbance at 280 nm using an Implen NP80 spectrophotometer (Implen, Munich, Germany).

Liquid Chromatography and MS

Peptides were analyzed on an EASY-nanoLC 1200 (Thermo Fisher Scientific, Bremen, Germany) coupled online to a Q Exactive HF mass spectrometer (Thermo Fisher Scientific). 1 μg of peptides were loaded on a μPAC trapping column (PharmaFluidics, Ghent, Belgium) at a flow rate of 2 μL/min

https://doi.org/10.1021/acs.jproteome.1c00783
J. Proteome Res. XXXX, XXX, XXX−XXX

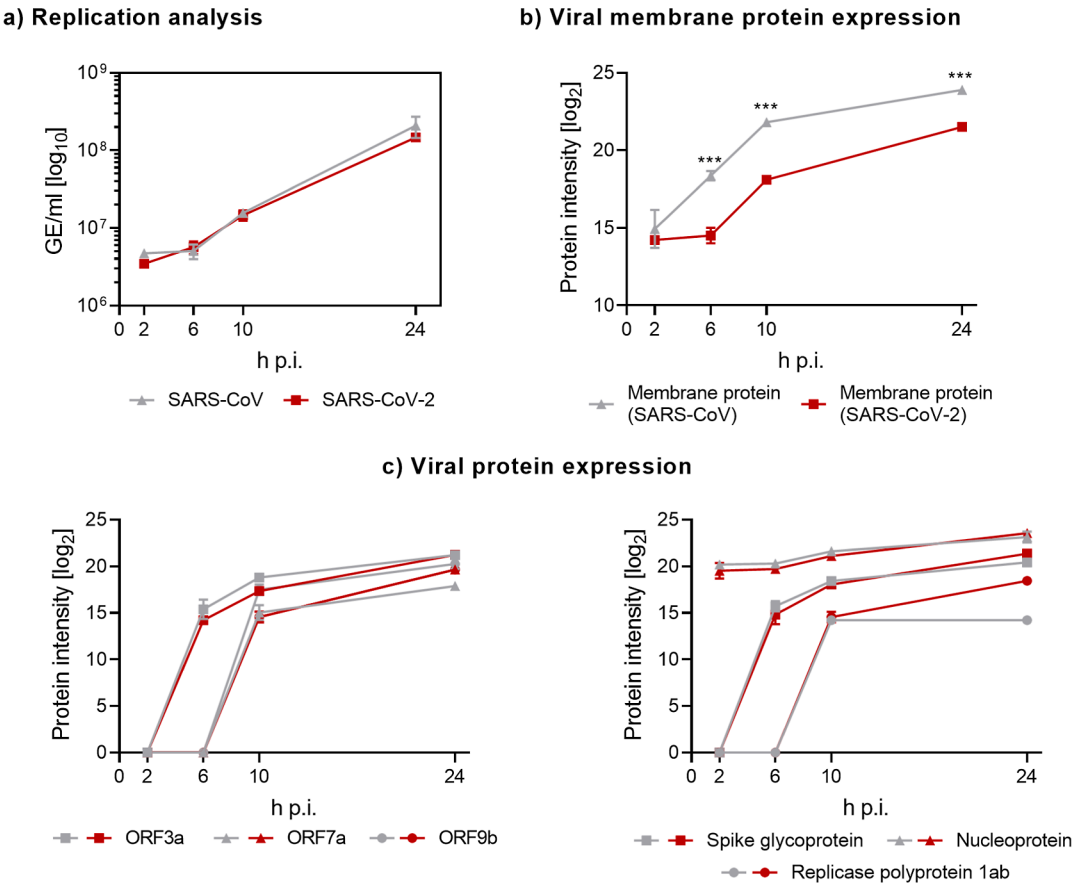

Figure 1. Viral protein expression and quantification of the virus in the supernatant. Calu-3 cells were infected with SARS-CoV, SARS-CoV-2, or mock-infected. (A) After 2, 6, 10, and 24 h p.i., the virus was quantified in the supernatant by qPCR. (B,C) Protein expression in infected cells was analyzed by DIA MS. Intensities of viral proteins in infected Calu-3 cells are shown. Intensities of non-detectable proteins were imputed using the minimal viral protein intensity. Statistical analysis was performed using a *t*-test, ***$p < 0.001$.

for 6 min and were subsequently separated on a 200 cm μPAC column (PharmaFluidics) using a stepped 160 min gradient of 80% acetonitrile (solvent B) in 0.1% formic acid (solvent A) at a 300 nL/min flow rate: 3−10% B for 22 min, 10−33% B for 95 min, 33−49% B for 23 min, 49−80% B for 10 min, and 80% B for 10 min. Column temperature was kept at 50 °C using a butterfly heater (Phoenix S&T, Chester, PA, USA). The Q Exactive HF was operated in a data-independent (DIA) manner in the m/z range of 350−1150. Full scan spectra were recorded with a resolution of 120,000 using an automatic gain control (AGC) target value of 3×10^6 with a maximum injection time of 100 ms. The full scans were followed by 84 DIA scans of dynamic window widths using an overlap of 0.5 Th (Supporting Information Table S1). For the correction of the predicted peptide spectral libraries, a pooled sample was measured using gas-phase separation (8 × 100 Th) with 25 × 4 Th windows in each fraction using a shift of 2 Th for subsequent cycles. Window placement was optimized using Skyline (Version 4.2.0).[12] DIA spectra were recorded at a resolution of 30,000 using an AGC target value of 3×10^6 with a maximum injection time of 55 ms and a first fixed mass of 200 Th. The normalized collision energy was set to 25%, and the default charge state was set to 3. Peptides were ionized using electrospray with a stainless-steel emitter, I.D. 30 μm (Proxeon, Odense, Denmark), at a spray voltage of 2.0 kV, and a heated capillary temperature of 275 °C.

Data Analysis

Protein sequences of *Homo sapiens* (UP000005640, 95,915 sequences, downloaded 23/5/19), SARS-CoV (UP000000354, 15 sequences, downloaded 21/9/20), and SARS-CoV-2 (UP000464024, 14 sequences, downloaded 21/9/20) were obtained from UniProt.[13] A combined spectral library was predicted for all possible peptides with strict trypsin specificity (KR not P) in the m/z range of 350−1150, with charge states of 2−4 and allowing up to one missed cleavage site using Prosit.[14] Input files for library prediction were generated using EncyclopeDIA (Version 0.9.5).[15] The *in silico* library was corrected using the data of the gas-phase fractionated pooled sample in DIA-NN (Version 1.7.10).[16] Mass tolerances were set to 10 ppm for MS1 and 20 ppm for MS^2 spectra, and the "unrelated run" option was enabled with the false discovery rate (FDR) being set to 0.01. The single-run data were analyzed using the corrected library with fixed mass tolerances of 10 ppm for MS1 and 20 ppm for MS^2 spectra with enabled "RT profiling" using the "robust LC (high accuracy)" quantification strategy. The FDR was set to 0.01 for precursor identifications, and proteins were grouped according to their respective genes. The resulting identification file was filtered using R (Version 3.6) in order to keep only proteotypic peptides and proteins with protein q-values < 0.01. Visualization and further analysis were done in Perseus (Version 1.6.5).[17] Relative protein quantification was done based on log (2)-transformed and Z-score normalized "MaxLFQ" intensities. Proteins which were not

https://doi.org/10.1021/acs.jproteome.1c00783
J. Proteome Res. XXXX, XXX, XXX−XXX

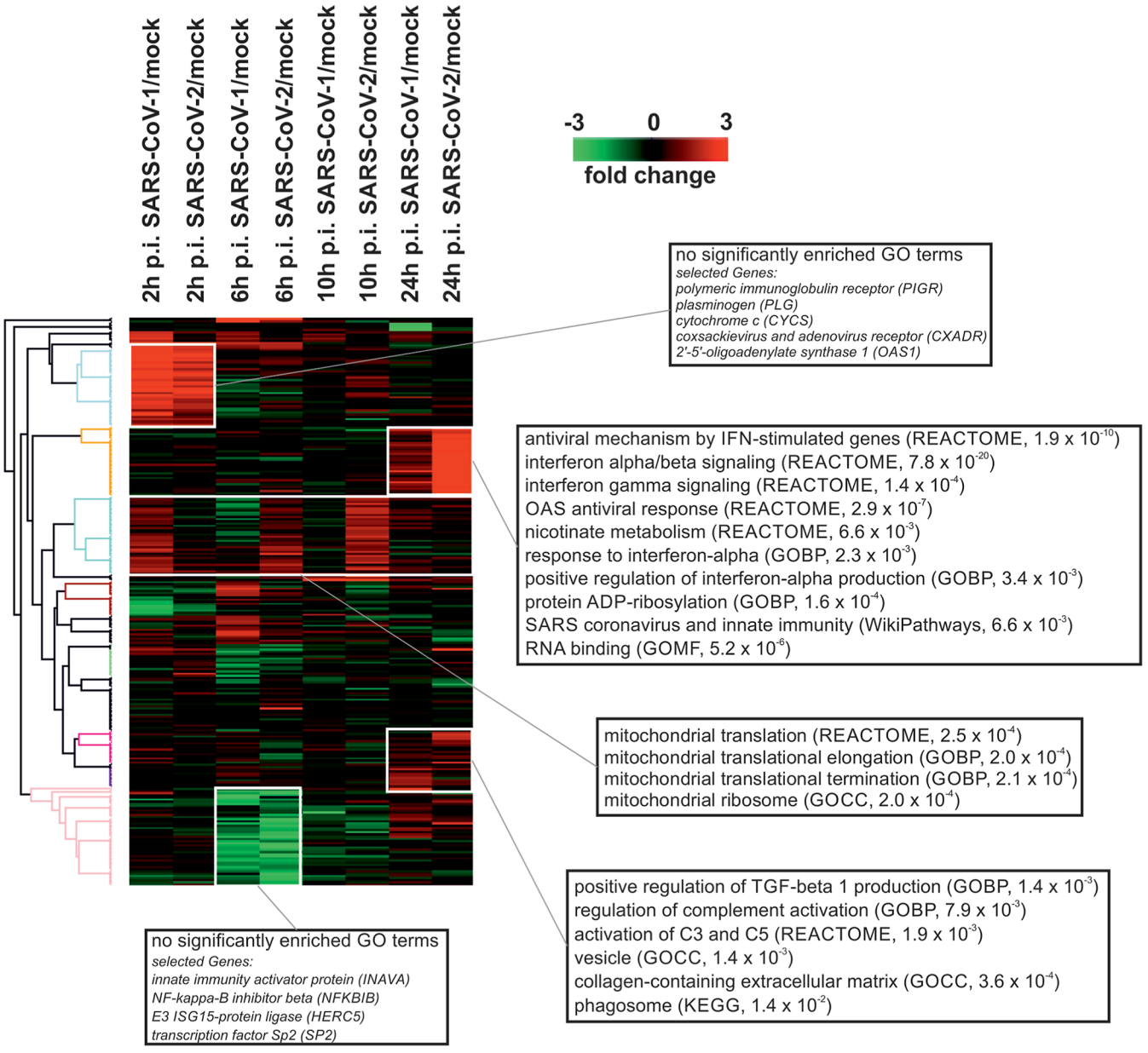

Figure 2. Infection-related alterations in the host proteome. Infection of Calu-3 cells with SARS-CoV and SARS-CoV-2 altered the abundance of 261 human proteins in comparison to time-matched mock controls. The heatmap depicts those proteins represented by their log2-transformed intensities using hierarchical clustering. Selected GO terms resulting from an enrichment analysis using ClueGO are denoted for the five main clusters. Complete results of the GO analysis can be found in the Supporting Information.

quantified in at least two-thirds of all samples were removed, and the remaining missing values were replaced from a normal distribution (width 0.3, down shift 1.8). Significant protein expression differences between samples were identified using an ANOVA test with a permutation-based FDR of 0.05 (250 randomizations, s0 = 1). Afterward, a post-hoc test was applied to detect significant sample pairs using an FDR of 0.05. Gene ontology enrichment of differentially expressed proteins was analyzed using the ClueGO app (Version 2.5.7) implemented in Cytoscape (Version 3.8.2) with a Bonferroni-adjusted *p*-value threshold of 0.05.[13,18,19]

RESULTS

Proteome Analysis of SARS-CoV- and SARS-CoV-2-Infected Calu-3 Cells

Proteome analysis of the SARS-CoV- and SARS-CoV-2-infected human lung epithelial cell line Calu-3 was conducted at 2, 6, 10, and 24 h p.i. including time-matched mock controls. Samples were prepared as biological triplicates and analyzed using single-shot DIA-based proteomics, with an optimized workflow for deep and accurate protein profiling.[20] In total, 8391 proteins were identified in a 3 h gradient, of which 7478 proteins were consistently quantified and used for further analysis (Pearson correlation >0.98, median coefficient of variation between 0.048 and 0.062 within each triplicate, data completeness 98.3%). Viral replication was verified by qPCR of the cell culture supernatants. The number of viral genome copies started to increase 6 h p.i.,

https://doi.org/10.1021/acs.jproteome.1c00783
J. Proteome Res. XXXX, XXX, XXX−XXX

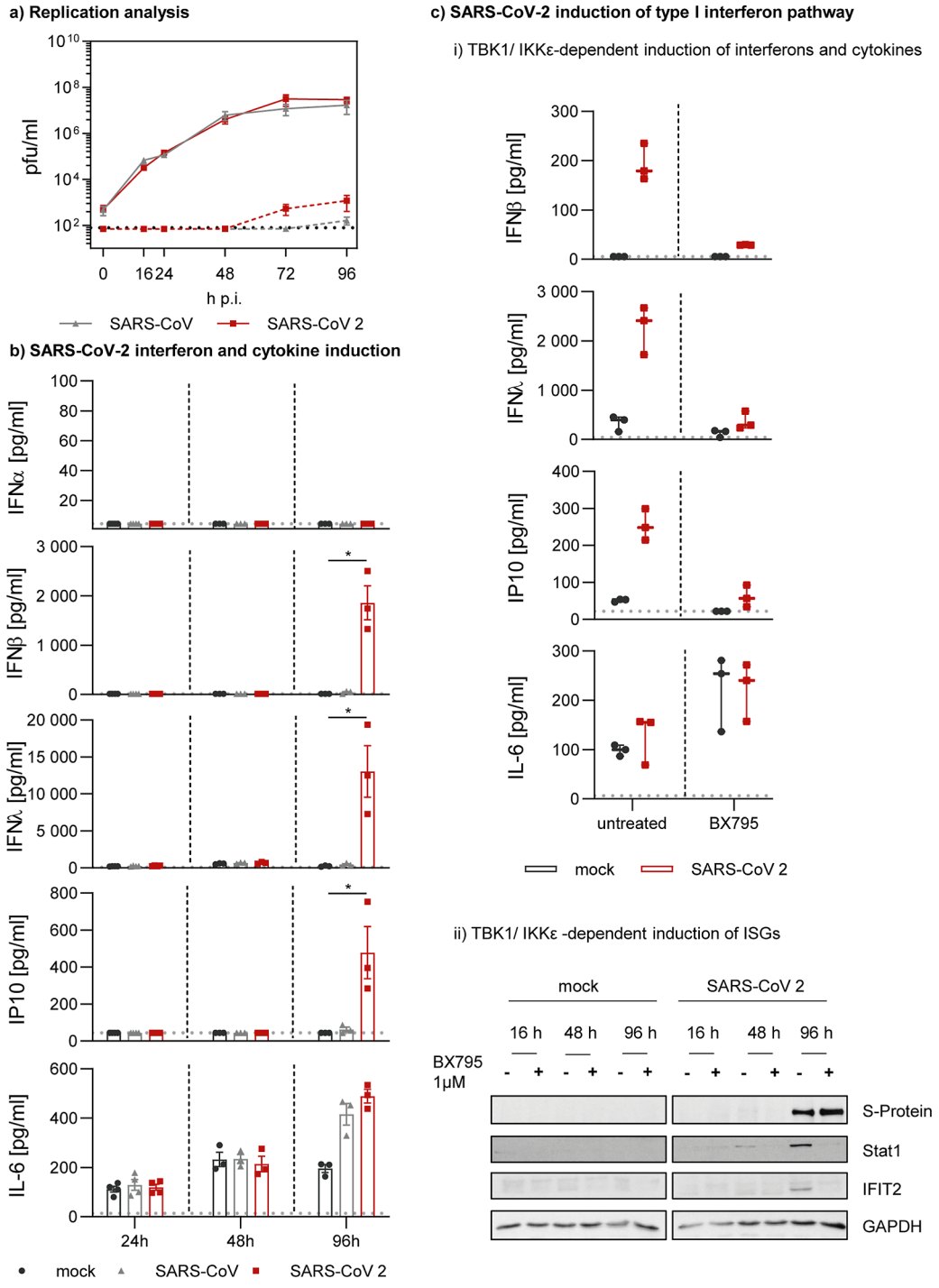

Figure 3. Induction of the type I IFN signaling pathway upon SARS-CoV-2 infection. (A) Replication analysis of SARS-CoV and SARS-CoV-2 was performed on polarized Calu-3 cells ($n = 3$ in duplicate). Calu-3 cells were infected at an MOI of 0.1, and supernatants from the apical and basolateral compartment were harvested at indicated time points. Solid lines represent samples taken from the apical site and dashed lines represent samples from the basolateral compartment. (B) Differentiated Calu-3 cells were infected mock or with SARS-CoV and SARS-CoV-2 at an MOI of 0.1. Supernatants from the apical compartment were harvested at indicated time points and analyzed regarding the designated interferons and cytokines. (C) Following pretreatment with 1 μM BX-795 for 6 h at 37 °C, Calu-3 cells were infected with SARS-CoV-2 at an MOI of 0.1. Supernatants were analyzed 96 h p.i. regarding the designated interferons and cytokines. At the indicated time points p.i., the cells were lysed and analyzed for the specified antigens using immunoblotting. Data are representative of two independent experiments. The limit of detection is shown by dotted lines (A–C). Statistical analysis was performed using the Kruskal–Wallis test (B) or the Mann–Whitney U test (C), $^*p < 0.05$.

and the replication between SARS-CoV and SARS-CoV-2 was comparable over the period of the experiment (Figure 1A). This is consistent with the expression of viral proteins, which was detectable from 6 h p.i. as well. The majority of viral proteins including nucleoprotein, spike glycoprotein, ORF3a, and ORF9a are not differentially expressed between SARS-CoV- and SARS-CoV-2-infected cells. An exception is the membrane protein (M) whose abundance is enhanced in SARS-CoV-infected cells compared to SARS-CoV-2-infected ones (Figure 1B,D, Supporting Information Tables S2 and S10).

https://doi.org/10.1021/acs.jproteome.1c00783
J. Proteome Res. XXXX, XXX, XXX−XXX

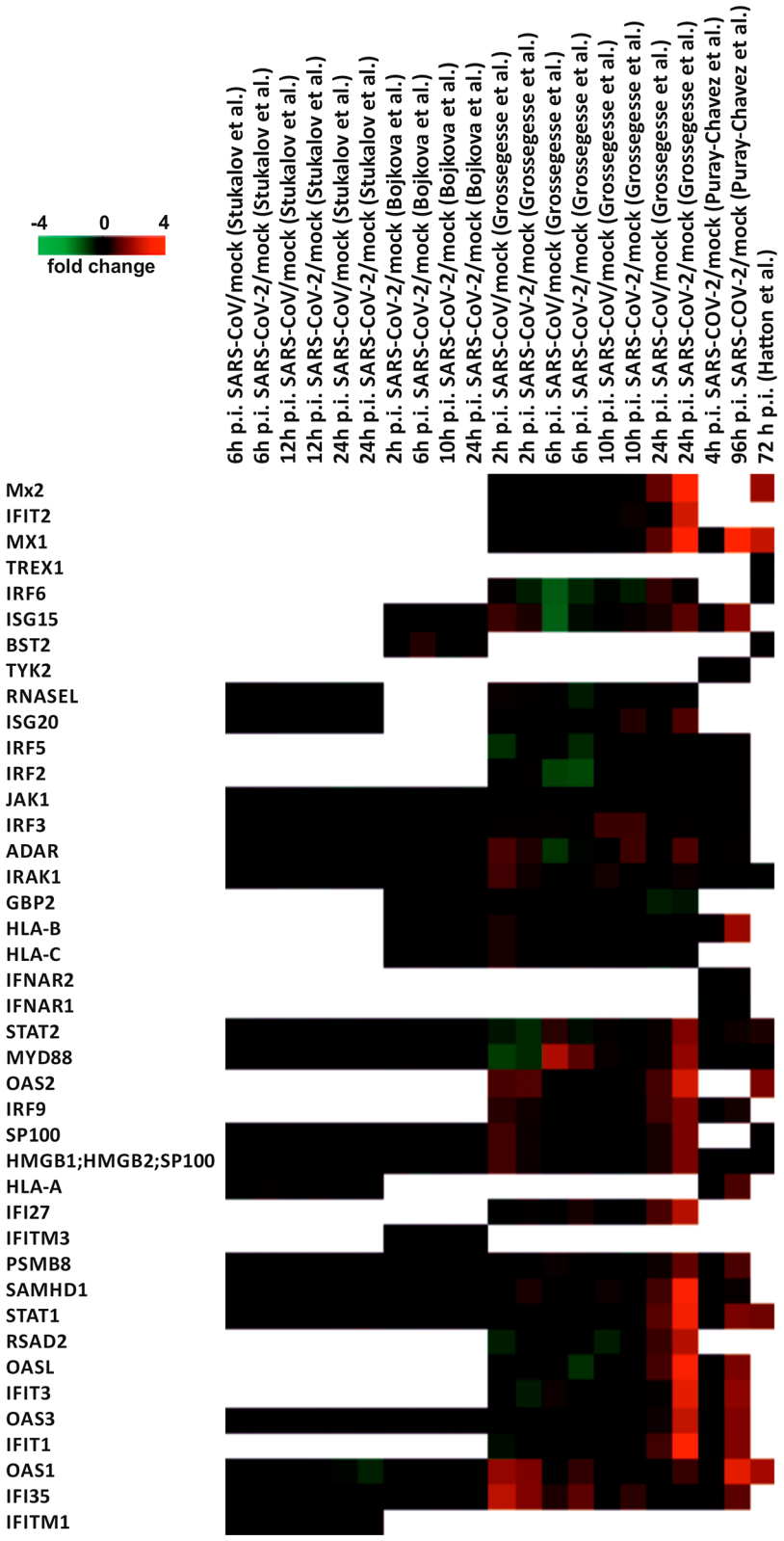

Figure 4. Comparative analysis of proteins associated with the type I IFN signaling pathway. Expression data of all identified proteins associated with the type I interferon signaling pathway (GO:0060337) were extracted from proteome studies of SARS-CoV-2-infected human cell lines done by Stukalov et al., Bojkova et al., Puray-Chavez et al., Hatton et al., and Grossegesse et al. and summarized in a heatmap representing log2-transformed intensity values. Missing values are in white.

The expression of 2642 human proteins differed significantly between the sample groups (ANOVA, FDR = 0.05), which was reduced to 261 proteins using a post-hoc test (FDR = 0.05) when only proteins with at least one significant pairwise difference in an infected cell with its time-matched mock control were kept (Supporting Information Table S3). This large

https://doi.org/10.1021/acs.jproteome.1c00783
J. Proteome Res. XXXX, XXX, XXX−XXX

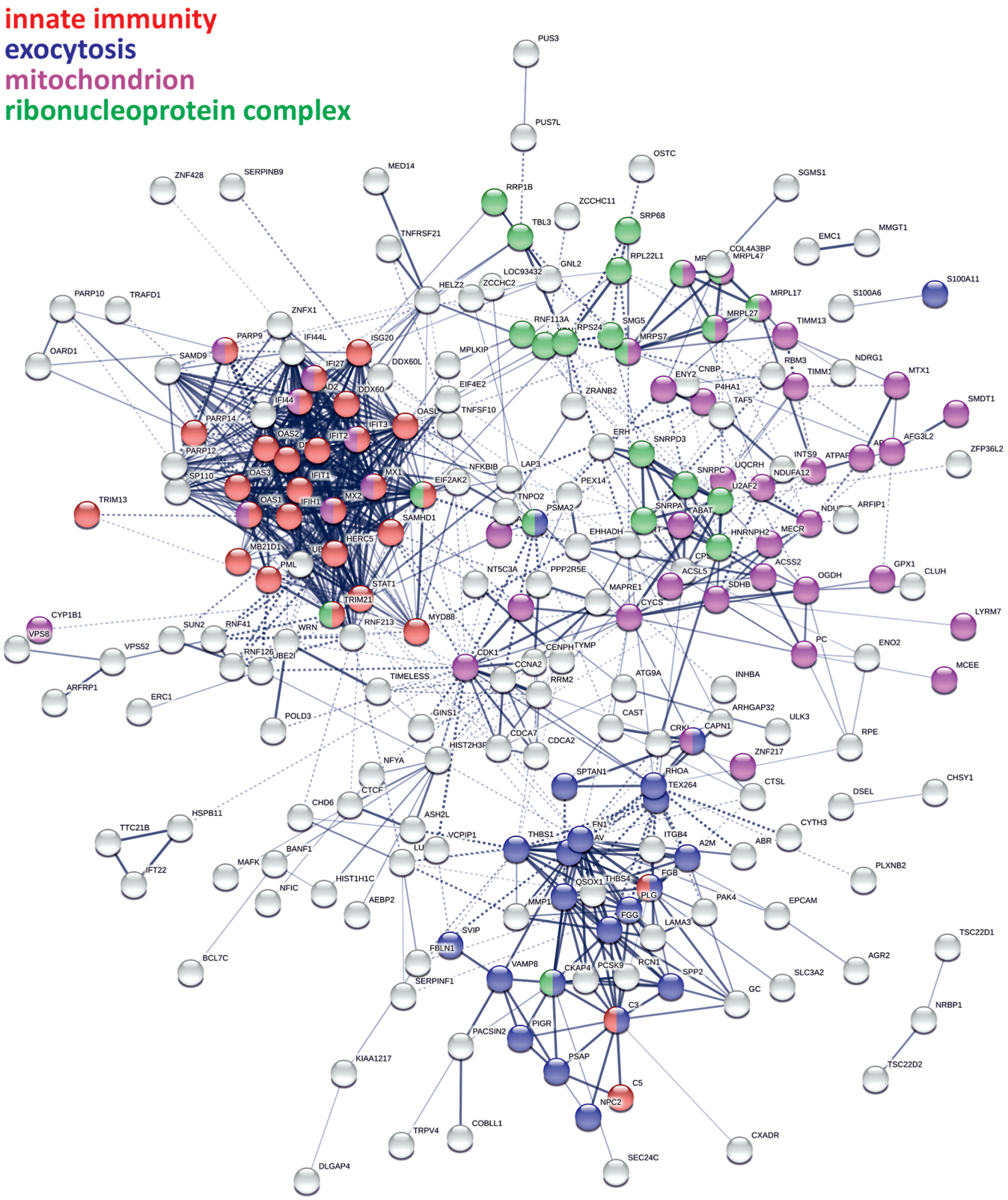

Figure 5. Protein interaction network of infection-related human proteins. The interaction network of all human proteins ($N = 261$), whose abundance in Calu-3 cells was altered by SARS-CoV and SARS-CoV-2 infection at any time p.i., was constructed using StringDB. The four major functional clusters, innate immunity, exocytosis, mitochondrion, and ribonucleoprotein complex, are color-coded. The tabular STRING output including all annotations is presented in Supporting Information Tables S7−S9.

reduction underlines the need for time-matched mock controls in viral proteomics because long incubation times themselves can already lead to large alterations of the cellular proteome. The remaining infection-related proteins were grouped using hierarchical clustering according to their expression profiles, and the respective main clusters were analyzed for enriched gene

https://doi.org/10.1021/acs.jproteome.1c00783
J. Proteome Res. XXXX, XXX, XXX−XXX

ontology terms using ClueGO (Figure 2 and Supporting Information Tables S4−S6). Out of the five clusters, two clusters (up-regulated 2 h p.i. and down-regulated 6 h p.i.) revealed no significantly enriched GO terms and among others contained several proteins related to immune response such as OAS1, INAVA, and NFKBIB. Another cluster consisting of proteins with virus-specific time-course-dependent upregulation was found to be related to mitochondrial translation (adjusted p-value: 2.5 * 10^{-4}, MRPL17, MRPL27, MRPL47, MRPL50, and MRPS7). The other two main clusters included upregulated proteins 24 h p.i. and are related to either the regulation of complement activation (adjusted p-value: 7.9 * 10^{-3}, C3 and C5) or interferon alpha/beta signaling (adjusted p-value: 7.8 * 10^{-20}, e.g., MX1, MX2, DDX58, STAT1, OAS2, OAS3, and IFIT3). Strikingly, the main difference between SARS-CoV- and SARS-CoV-2-infected cells was observed for proteins derived from ISGs, whose expression is enhanced in SARS-CoV-2-infected cells in comparison to SARS-CoV infection.

Verification of Enhanced IFN Induction by SARS-CoV-2

The induction of the type I IFN response was further validated in differentiated Calu-3 cell ALI cultures, which mimic the human respiratory tract more closely in comparison to non-polarized cell systems. SARS-CoV and SARS-CoV-2 replicated in differentiated Calu-3 cells to similar high viral titers of about 10^8 plaque-forming units per milliliter peaking at 72 h p.i (Figure 3A). IFN β and -λ and the IFN-induced chemokine IP-10 were detected at late time points specifically in supernatants of cells following infection with SARS-CoV-2 but not SARS-CoV (Figure 3B), which is in line with the selective upregulation of ISGs following SARS-CoV-2 infection observed in the proteome analysis (Figure 2). In contrast to IFNs, pro-inflammatory cytokines, as exemplified by IL-6, were induced by both viruses. RNA viruses such as SARS-CoV-2 are recognized by the innate immune system via the cytoplasmic double-stranded RNA (dsRNA) sensors RIG-I and MDA5, which signal via the adaptor protein MAVS to induce the expression of IFNs and pro-inflammatory cytokines.[21] Activation of MAVS leads to the recruitment and activation of the downstream kinases TBK1/IKKε, which in turn regulate the expression of IFNs via phosphorylation and activation of IRF 3. Interestingly, treatment of SARS-CoV-2-infected cells with BX-795, an inhibitor of IKKε and TBK1, strongly reduced the expression of IFNβ and IFNλ and of the ISGs IP-10, IFIT 2, and STAT 1 (Figure 3C), indicating an IKKε- or TBK1-dependency of the IFN response induced following SARS-CoV-2 infection. At the same time, induction of IL-6 remained unchanged. IFN-induction by SARS-CoV-2 was further analyzed in ACE2-A549 reporter cells, confirming a higher IRF activity in SARS-CoV-2-infected cells compared to no detectable IRF activity upon infection with SARS-CoV (Supporting Information Figure S1).

Comparison of Proteome Studies Analyzing the SARS-CoV-2 IFN Response

As the type I IFN response is one of the most important responses of the innate immune system to RNA viruses, we compared the expression data of related proteins from this study with other proteome studies of SARS-CoV-2-infected human cells. The selection was based on data availability (Supporting Information Table S11). For this purpose, all identified proteins annotated with the GO term "type I interferon signaling pathway" (GO:0060337) were extracted from the data of Stukalov et al. (A549-ACE2 cells, MOI = 2), Bojkova et al. (Caco-2 cells, MOI = 1), Puray-Chavez et al. (H552 cells, MOI = 1), and Hatton et al. (primary human nasal airway epithelial cells, MOI = 0.1) and matched and clustered according to their expression profiles (Figure 4).[22−25] The resulting heatmap revealed that the activation of the type I IFN response is completely absent in the studies of Bojkova et al. and Stukalov et al. However, it has to be noted that the coverage of this pathway differs strongly among the studies. Most of the ISGs with expression changes induced by infection are not detected in these two studies. Interestingly, the study of Puray-Chavez et al. detected a similar increase of ISG abundance 96 h p.i. in H522 cells, which are human lung epithelial cells derived from adenocarcinoma tissue, as Calu-3 cells, which were analyzed in this study. Furthermore, an interaction network of all proteins, whose abundance was significantly altered in Calu-3 cells by infection (N = 261), was constructed using STRING (ref 26, https://string-db.org/) (Figure 5 and Supporting Information Tables S7−S9). The network revealed high connectivity among proteins related to either innate immunity (mainly type I IFN signaling), exocytosis, including proteins related to platelet degranulation (adjusted p-value: 0.01, e.g., FGB, FGG, FN1, PLG, and PSAP) or mitochondria-associated proteins including many members of ribonucleoprotein complexes, among them five members of the mitochondrial ribosome (MRPL17, MRPL27, MRPL47, MRPL50, and MRPS7).

DISCUSSION

Innate immunity is the host's first line of defence to fight infections. One of the most important mechanisms to combat replication of RNA viruses is the interferon response. It is based on the recognition of pathogen-associated molecular patterns, especially dsRNA, which in the end results in the secretion of type I IFNs, which in turn induce the expression of ISGs including multiple antiviral proteins.[27] SARS-CoV-2 is more susceptible to both IFN-α and IFN-β treatment in cultured cells than SARS-CoV,[28−31] which is why type I IFNs could be a possible treatment for COVID-19.[32] Data from SARS-CoV-2-infected patients report low or absent levels of IFN-I in serum but induction of ISG expression.[3,33] In this study, protein expression of SARS-CoV- and SARS-CoV-2-infected Calu-3 cells was analyzed, which should be well suited to uncover the modulation of the type I IFN response during infection. This analysis resulted in a comprehensive proteome map of SARS-CoV- and SARS-CoV-2-infected Calu-3 cells covering ∼7400 proteins across four time points. Expression of 261 proteins changed during the course of infection, which cluster into five main groups. One of those clusters reveals a strong induction of ISG expression 24 h p.i. in SARS-CoV-2-infected cells. Strikingly, this induction was observed at a much lower level in SARS-CoV-infected cells. Among those ISG proteins is, for example, the interferon-induced GTP-binding protein MX1, which is known for its antiviral activity against a wide range of mainly RNA viruses. MX1 expression is increased in SARS-CoV-2-infected patients and correlates well with viral load.[34] Furthermore, ISG expression is induced in SARS-CoV-2-infected patients in general and the increase of ISG expression, including MX1, negatively correlates with disease severity.[33] Surprisingly, these findings are not well reflected in the current literature of large-scale proteome analysis of infected human cells and are completely absent in two studies.[22,23] The absence of an enhanced ISG expression in other proteome studies can result from incomplete proteome coverage or from different experimental conditions, for example, different cell lines and MOIs.[35,36] It was shown before that ISGs and IFN can be

https://doi.org/10.1021/acs.jproteome.1c00783
J. Proteome Res. XXXX, XXX, XXX−XXX

detected upon infection of A549-ACE2 and Calu-3 cells with SARS-CoV-2 and that higher MOIs favor interferon induction.[35,36] However, this was surprisingly not detected in the study of Stukalov et al. To shed light on this discrepancy, we performed a comparative analysis of type I IFN-related proteins by comparing data from this study to four other proteomic studies of SARS-CoV-2-infected human cells.[22−25] Interestingly, most of the strongly affected ISGs, including MX1, MX2, IFIT1, IFIT2, IFIT3, OASL, and OASL2, were not identified in these studies except by Puray-Chavez et al. This study supports our findings for SARS-COV-2 induction of expression of the aforementioned ISGs in another human lung cell line quite well. The low coverage of this pathway in the other studies could explain at least partially the discrepancy. It should also be noted that ACE2 is an ISG itself and the influence of ACE2 overexpression, which was used by Stukalov et al. to turn A549 into a permissive cell line, on the immune response is unknown.[7] This comparative analysis demonstrates that proteome coverage is still a limitation which impedes inter-study comparisons due to missing values.

Recently, it was proposed that SARS-CoV-2 ORF6 interferes less efficiently with human IFN induction and IFN signaling than SARS-CoV ORF6, which could explain the virus-specific induction of ISG expression and the varying IFN sensitivity.[37] The proteome data from this study point toward an additional mechanism. The abundance of viral proteins was highly similar between SARS-CoV and SARS-CoV-2 except for the M protein whose abundance is enhanced in SARS-CoV. This protein is a component of the viral envelope, but its functions beyond are not well characterized. It is known that the homologous M proteins of MERS and SARS-CoV inhibit type I IFN expression.[38,39] Overexpression of the M protein from SARS-CoV-2 in human cells inhibits the production of type I and III IFNs induced by dsRNA-sensing via direct interaction with RIG-I (DDX58) and reduces the induction of ISGs after Sendai virus infection and poly (I/C) transfection.[36,40] Additionally, the M protein of SARS-CoV inhibits the formation of the TRAF3−TANK−TBK1/IKKε complex, resulting in the inhibition of IFN transcription.[38] In line with these findings, we were able to show that the induction of type I IFN induced following SARS-CoV-2 infection is dependent on the TBKI pathway as well (Figure 3c). We therefore hypothesize that the enhanced abundance of the M protein of SARS-CoV reduces the induction of ISG expression in infected cells in comparison to SARS-CoV-2 and thereby contributes to the varying IFN sensitivity of both viruses. However, it should be noted that also sequence differences in the M protein of both viruses (amino acid identity = 90.5%) could lead to differences in the IFN-antagonizing capacity, which is not known so far.

In summary, this study presents the so far most comprehensive comparative quantitative proteomics data set of SARS-CoV- and SARS-CoV-2-infected Calu-3 cells, which are the only permissive human lung cell line for SARS-CoV-2.[6] By showing a diverse regulation of ISG expression upon infection, we conclude that Calu-3 cells present a good model system for studying differences in IFN sensitivity of SARS-CoV and SARS-CoV-2.

■ ASSOCIATED CONTENT

Supporting Information

The Supporting Information is available free of charge at https://pubs.acs.org/doi/10.1021/acs.jproteome.1c00783.

Cytopathic effect and IRF activity (PDF)

DIA Windows; ClueGO Result Human Cluster 1; ClueGO Result Human Cluster 2; ClueGO Result Human Cluster 3; STRING enrichment (biological process); STRING enrichment (molecular function); STRING enrichment (cellular compartment); human proteins affected by infection (log2 transformed); viral protein expression (mean log2 values); protein output; global proteome expression studies of SARS-CoV-2-infected human cell lines (XLSX)

■ AUTHOR INFORMATION

Corresponding Author

Joerg Doellinger − *Centre for Biological Threats and Special Pathogens: Highly Pathogenic Viruses (ZBS 1) and Centre for Biological Threats and Special Pathogens: Proteomics and Spectroscopy (ZBS 6), Robert Koch Institute, 13353 Berlin, Germany;* orcid.org/0000-0001-8309-082X; Phone: 49-30-18754-2373; Email: Doellingerj@rki.de

Authors

Marica Grossegesse − *Centre for Biological Threats and Special Pathogens: Highly Pathogenic Viruses (ZBS 1), Robert Koch Institute, 13353 Berlin, Germany;* orcid.org/0000-0002-9369-8203

Daniel Bourquain − *Centre for Biological Threats and Special Pathogens, Robert Koch Institute, 13353 Berlin, Germany*

Markus Neumann − *Centre for Biological Threats and Special Pathogens: Highly Pathogenic Viruses (ZBS 1), Robert Koch Institute, 13353 Berlin, Germany*

Lars Schaade − *Centre for Biological Threats and Special Pathogens, Robert Koch Institute, 13353 Berlin, Germany*

Jessica Schulze − *Influenza and Other Respiratory Viruses, Robert Koch Institute, 13353 Berlin, Germany*

Christin Mache − *Influenza and Other Respiratory Viruses, Robert Koch Institute, 13353 Berlin, Germany*

Thorsten Wolff − *Influenza and Other Respiratory Viruses, Robert Koch Institute, 13353 Berlin, Germany;* orcid.org/0000-0001-7688-236X

Andreas Nitsche − *Centre for Biological Threats and Special Pathogens: Highly Pathogenic Viruses (ZBS 1), Robert Koch Institute, 13353 Berlin, Germany*

Complete contact information is available at: https://pubs.acs.org/10.1021/acs.jproteome.1c00783

Notes

The authors declare no competing financial interest.

The MS proteomics data have been deposited to the ProteomeXchange Consortium (http://proteomecentral.proteomexchange.org) via the PRIDE partner repository with the data set identifiers PXD024883.

■ ACKNOWLEDGMENTS

The authors would like to thank Clemens Bodenstein, Bianca Hube, Melanie Hoffmeister, and Stefanie Schürer for supporting the infection experiments and qPCR and Ursula Erikli for copy-editing. This work was supported in part by grants from the Federal Ministry of Health (SynSARICO) and the Federal Ministry of Education and Research [grant 01KI2006A (RAPID)]. The graphical abstract was created with BioRender.com.

https://doi.org/10.1021/acs.jproteome.1c00783
J. Proteome Res. XXXX, XXX, XXX−XXX

REFERENCES

(1) Hui, D. S.; Azhar, E.; Madani, T. A.; Ntoumi, F.; Kock, R.; Dar, O.; Ippolito, G.; McHugh, T. D.; Memish, Z. A.; Drosten, C.; Zumla, A.; Petersen, E. The continuing 2019-nCoV epidemic threat of novel coronaviruses to global health - The latest 2019 novel coronavirus outbreak in Wuhan, China. *Int. J. Infect. Dis.* **2020**, *91*, 264−266.

(2) Petersen, E.; Koopmans, M.; Go, U.; Hamer, D. H.; Petrosillo, N.; Castelli, F.; Storgaard, M.; Al Khalili, S.; Simonsen, L. Comparing SARS-CoV-2 with SARS-CoV and influenza pandemics. *Lancet Infect. Dis.* **2020**, *20*, e238−e244.

(3) Chan, J. F.-W.; Kok, K.-H.; Zhu, Z.; Chu, H.; To, K. K.-W.; Yuan, S.; Yuen, K.-Y. Genomic characterization of the 2019 novel human-pathogenic coronavirus isolated from a patient with atypical pneumonia after visiting Wuhan. *Emerg. Microb. Infect.* **2020**, *9*, 221−236.

(4) Grifoni, A.; Sidney, J.; Zhang, Y.; Scheuermann, R. H.; Peters, B.; Sette, A. A Sequence Homology and Bioinformatic Approach Can Predict Candidate Targets for Immune Responses to SARS-CoV-2. *Cell Host Microbe* **2020**, *27*, 671−680.

(5) Rossi, G. A.; Sacco, O.; Mancino, E.; Cristiani, L.; Midulla, F. Differences and similarities between SARS-CoV and SARS-CoV-2: spike receptor-binding domain recognition and host cell infection with support of cellular serine proteases. *Infection* **2020**, *48*, 665−669.

(6) Cagno, V. SARS-CoV-2 cellular tropism. *Lancet Microbe* **2020**, *1*, e2−e3.

(7) Ziegler, C. G. K.; Allon, S. J.; Nyquist, S. K.; Mbano, I. M.; Miao, V. N.; Tzouanas, C. N.; Cao, Y.; Yousif, A. S.; Bals, J.; Hauser, B. M.; Feldman, J.; Muus, C.; Wadsworth, M. H., 2nd; Kazer, S. W.; Hughes, T. K.; Doran, B.; Gatter, G. J.; Vukovic, M.; Taliaferro, F.; Mead, B. E.; Guo, Z.; Wang, J. P.; Gras, D.; Plaisant, M.; Ansari, M.; Angelidis, I.; Adler, H.; Sucre, J. M. S.; Taylor, C. J.; Lin, B.; Waghray, A.; Mitsialis, V.; Dwyer, D. F.; Buchheit, K. M.; Boyce, J. A.; Barrett, N. A.; Laidlaw, T. M.; Carroll, S. L.; Colonna, L.; Tkachev, V.; Peterson, C. W.; Yu, A.; Zheng, H. B.; Gideon, H. P.; Winchell, C. G.; Lin, P. L.; Bingle, C. D.; Snapper, S. B.; Kropski, J. A.; Theis, F. J.; Schiller, H. B.; Zaragosi, L.-E.; Barbry, P.; Leslie, A.; Kiem, H.-P.; Flynn, J. L.; Fortune, S. M.; Berger, B.; Finberg, R. W.; Kean, L. S.; Garber, M.; Schmidt, A. G.; Lingwood, D.; Shalek, A. K.; Ordovas-Montanes, J.; Banovich, N.; Barbry, P.; Brazma, A.; Desai, T.; Duong, T. E.; Eickelberg, O.; Falk, C.; Farzan, M.; Glass, I.; Haniffa, M.; Horvath, P.; Hung, D.; Kaminski, N.; Krasnow, M.; Kropski, J. A.; Kuhnemund, M.; Lafyatis, R.; Lee, H.; Leroy, S.; Linnarson, S.; Lundeberg, J.; Meyer, K.; Misharin, A.; Nawijn, M.; Nikolic, M. Z.; Ordovas-Montanes, J.; Pe'er, D.; Powell, J.; Quake, S.; Rajagopal, J.; Tata, P. R.; Rawlins, E. L.; Regev, A.; Reyfman, P. A.; Rojas, M.; Rosen, O.; Saeb-Parsy, K.; Samakovlis, C.; Schiller, H.; Schultze, J. L.; Seibold, M. A.; Shalek, A. K.; Shepherd, D.; Spence, J.; Spira, A.; Sun, X.; Teichmann, S.; Theis, F.; Tsankov, A.; van den Berge, M.; von Papen, M.; Whitsett, J.; Xavier, R.; Xu, Y.; Zaragosi, L.-E.; Zhang, K. SARS-CoV-2 Receptor ACE2 Is an Interferon-Stimulated Gene in Human Airway Epithelial Cells and Is Detected in Specific Cell Subsets across Tissues. *Cell* **2020**, *181*, 1016−1035.

(8) Michel, J.; Neumann, M.; Krause, E.; Rinner, T.; Muzeniek, T.; Grossegesse, M.; Hille, G.; Schwarz, F.; Puyskens, A.; Förster, S.; Biere, B.; Bourquain, D.; Domingo, C.; Brinkmann, A.; Schaade, L.; Schrick, L.; Nitsche, A. Resource-efficient internally controlled in-house real-time PCR detection of SARS-CoV-2. *Virol. J.* **2021**, *18*, 110.

(9) Corman, V. M.; Landt, O.; Kaiser, M.; Molenkamp, R.; Meijer, A.; Chu, D. K.; Bleicker, T.; Brunink, S.; Schneider, J.; Schmidt, M. L.; Mulders, D. G.; Haagmans, B. L.; van der Veer, B.; van den Brink, S.; Wijsman, L.; Goderski, G.; Romette, J. L.; Ellis, J.; Zambon, M.; Peiris, M.; Goossens, H.; Reusken, C.; Koopmans, M. P.; Drosten, C., Detection of 2019 novel coronavirus (2019-nCoV) by real-time RT-PCR. *Euro Surveill.***2020**, *25* . DOI: 10.2807/1560-7917.es.2020.25.3.2000045

(10) Doellinger, J.; Schneider, A.; Hoeller, M.; Lasch, P. Sample Preparation by Easy Extraction and Digestion (SPEED) - A Universal, Rapid, and Detergent-free Protocol for Proteomics Based on Acid Extraction. *Mol. Cell. Proteomics* **2020**, *19*, 209−222.

(11) Rappsilber, J.; Mann, M.; Ishihama, Y. Protocol for micro-purification, enrichment, pre-fractionation and storage of peptides for proteomics using StageTips. *Nat. Protoc.* **2007**, *2*, 1896−1906.

(12) Pino, L. K.; Searle, B. C.; Bollinger, J. G.; Nunn, B.; MacLean, B.; MacCoss, M. J. The Skyline ecosystem: Informatics for quantitative mass spectrometry proteomics. *Mass Spectrom. Rev.* **2020**, *39*, 229−244.

(13) UniProt, C. UniProt: a worldwide hub of protein knowledge. *Nucleic Acids Res.* **2019**, *47*, D506−D515.

(14) Gessulat, S.; Schmidt, T.; Zolg, D. P.; Samaras, P.; Schnatbaum, K.; Zerweck, J.; Knaute, T.; Rechenberger, J.; Delanghe, B.; Huhmer, A.; Reimer, U.; Ehrlich, H.-C.; Aiche, S.; Kuster, B.; Wilhelm, M. Prosit: proteome-wide prediction of peptide tandem mass spectra by deep learning. *Nat. Methods* **2019**, *16*, 509−518.

(15) Searle, B. C.; Pino, L. K.; Egertson, J. D.; Ting, Y. S.; Lawrence, R. T.; MacLean, B. X.; Villén, J.; MacCoss, M. J. Chromatogram libraries improve peptide detection and quantification by data independent acquisition mass spectrometry. *Nat. Commun.* **2018**, *9*, 5128.

(16) Demichev, V.; Messner, C. B.; Vernardis, S. I.; Lilley, K. S.; Ralser, M. DIA-NN: neural networks and interference correction enable deep proteome coverage in high throughput. *Nat. Methods* **2020**, *17*, 41−44.

(17) Tyanova, S.; Temu, T.; Sinitcyn, P.; Carlson, A.; Hein, M. Y.; Geiger, T.; Mann, M.; Cox, J. The Perseus computational platform for comprehensive analysis of (prote)omics data. *Nat. Methods* **2016**, *13*, 731−740.

(18) Bindea, G.; Mlecnik, B.; Hackl, H.; Charoentong, P.; Tosolini, M.; Kirilovsky, A.; Fridman, W.-H.; Pagès, F.; Trajanoski, Z.; Galon, J. ClueGO: a Cytoscape plug-in to decipher functionally grouped gene ontology and pathway annotation networks. *Bioinformatics* **2009**, *25*, 1091−1093.

(19) Shannon, P.; Markiel, A.; Ozier, O.; Baliga, N. S.; Wang, J. T.; Ramage, D.; Amin, N.; Schwikowski, B.; Ideker, T. Cytoscape: a software environment for integrated models of biomolecular interaction networks. *Genome Res.* **2003**, *13*, 2498−2504.

(20) Doellinger, J.; Blumenscheit, C.; Schneider, A.; Lasch, P. Isolation Window Optimization of Data-Independent Acquisition Using Predicted Libraries for Deep and Accurate Proteome Profiling. *Anal. Chem.* **2020**, *92*, 12185−12192.

(21) Thorne, L. G.; Reuschl, A. K.; Zuliani-Alvarez, L.; Whelan, M. V. X.; Turner, J.; Noursadeghi, M.; Jolly, C.; Towers, G. J. SARS-CoV-2 sensing by RIG-I and MDA5 links epithelial infection to macrophage inflammation. *EMBO J.* **2021**, *40*, No. e107826.

(22) Stukalov, A.; Girault, V.; Grass, V.; Karayel, O.; Bergant, V.; Urban, C.; Haas, D. A.; Huang, Y.; Oubraham, L.; Wang, A.; Hamad, M. S.; Piras, A.; Hansen, F. M.; Tanzer, M. C.; Paron, I.; Zinzula, L.; Engleitner, T.; Reinecke, M.; Lavacca, T. M.; Ehmann, R.; Wölfel, R.; Jores, J.; Kuster, B.; Protzer, U.; Rad, R.; Ziebuhr, J.; Thiel, V.; Scaturro, P.; Mann, M.; Pichlmair, A. Multilevel proteomics reveals host perturbations by SARS-CoV-2 and SARS-CoV. *Nature* **2021**, *594*, 246−252.

(23) Bojkova, D.; Klann, K.; Koch, B.; Widera, M.; Krause, D.; Ciesek, S.; Cinatl, J.; Münch, C. Proteomics of SARS-CoV-2-infected host cells reveals therapy targets. *Nature* **2020**, *583*, 469−472.

(24) Puray-Chavez, M.; LaPak, K. M.; Schrank, T. P.; Elliott, J. L.; Bhatt, D. P.; Agajanian, M. J.; Jasuja, R.; Lawson, D. Q.; Davis, K.; Rothlauf, P. W.; Liu, Z.; Jo, H.; Lee, N.; Tenneti, K.; Eschbach, J. E.; Shema Mugisha, C.; Cousins, E. M.; Cloer, E. W.; Vuong, H. R.; VanBlargan, L. A.; Bailey, A. L.; Gilchuk, P.; Crowe, J. E., Jr.; Diamond, M. S.; Hayes, D. N.; Whelan, S. P. J.; Horani, A.; Brody, S. L.; Goldfarb, D.; Major, M. B.; Kutluay, S. B. Systematic analysis of SARS-CoV-2 infection of an ACE2-negative human airway cell. *Cell Rep.* **2021**, *36*, 109364.

(25) Hatton, C. F.; Botting, R. A.; Dueñas, M. E.; Haq, I. J.; Verdon, B.; Thompson, B. J.; Spegarova, J. S.; Gothe, F.; Stephenson, E.; Gardner, A. I.; Murphy, S.; Scott, J.; Garnett, J. P.; Carrie, S.; Powell, J.; Khan, C. M. A.; Huang, L.; Hussain, R.; Coxhead, J.; Davey, T.; Simpson, A. J.; Haniffa, M.; Hambleton, S.; Brodlie, M.; Ward, C.; Trost, M.; Reynolds, G.; Duncan, C. J. A. Delayed induction of type I

https://doi.org/10.1021/acs.jproteome.1c00783
J. Proteome Res. XXXX, XXX, XXX−XXX

and III interferons mediates nasal epithelial cell permissiveness to SARS-CoV-2. *bioRxiv* **2021**, DOI: 10.1038/s41467-021-27318-0.
(26) Jensen, L. J.; Kuhn, M.; Stark, M.; Chaffron, S.; Creevey, C.; Muller, J.; Doerks, T.; Julien, P.; Roth, A.; Simonovic, M.; Bork, P.; von Mering, C. STRING 8–a global view on proteins and their functional interactions in 630 organisms. *Nucleic Acids Res.* **2009**, *37*, D412.
(27) Mesev, E. V.; LeDesma, R. A.; Ploss, A. Decoding type I and III interferon signalling during viral infection. *Nat. Microbiol.* **2019**, *4*, 914−924.
(28) Lokugamage, K. G.; Hage, A.; de Vries, M.; Valero-Jimenez, A. M.; Schindewolf, C.; Dittmann, M.; Rajsbaum, R.; Menachery, V. D., Type I Interferon Susceptibility Distinguishes SARS-CoV-2 from SARS-CoV. *J. Virol.***2020**, *94*. DOI: 10.1128/JVI.01410-20
(29) Mantlo, E.; Bukreyeva, N.; Maruyama, J.; Paessler, S.; Huang, C. Antiviral activities of type I interferons to SARS-CoV-2 infection. *Antiviral Res.* **2020**, *179*, 104811.
(30) Shuai, H.; Chu, H.; Hou, Y.; Yang, D.; Wang, Y.; Hu, B.; Huang, X.; Zhang, X.; Chai, Y.; Cai, J.-P.; Chan, J. F.-W.; Yuen, K.-Y. Differential immune activation profile of SARS-CoV-2 and SARS-CoV infection in human lung and intestinal cells: Implications for treatment with IFN-beta and IFN inducer. *J. Infect.* **2020**, *81*, e1−e10.
(31) Felgenhauer, U.; Schoen, A.; Gad, H. H.; Hartmann, R.; Schaubmar, A. R.; Failing, K.; Drosten, C.; Weber, F. Inhibition of SARS-CoV-2 by type I and type III interferons. *J. Biol. Chem.* **2020**, *295*, 13958−13964.
(32) Sa Ribero, M.; Jouvenet, N.; Dreux, M.; Nisole, S. Interplay between SARS-CoV-2 and the type I interferon response. *PLoS Pathog.* **2020**, *16*, No. e1008737.
(33) Hadjadj, J.; Yatim, N.; Barnabei, L.; Corneau, A.; Boussier, J.; Smith, N.; Péré, H.; Charbit, B.; Bondet, V.; Chenevier-Gobeaux, C.; Breillat, P.; Carlier, N.; Gauzit, R.; Morbieu, C.; Pène, F.; Marin, N.; Roche, N.; Szwebel, T.-A.; Merkling, S. H.; Treluyer, J.-M.; Veyer, D.; Mouthon, L.; Blanc, C.; Tharaux, P.-L.; Rozenberg, F.; Fischer, A.; Duffy, D.; Rieux-Laucat, F.; Kernéis, S.; Terrier, B. Impaired type I interferon activity and inflammatory responses in severe COVID-19 patients. *Science* **2020**, *369*, 718−724.
(34) Bizzotto, J.; Sanchis, P.; Abbate, M.; Lage-Vickers, S.; Lavignolle, R.; Toro, A.; Olszevicki, S.; Sabater, A.; Cascardo, F.; Vazquez, E.; Cotignola, J.; Gueron, G. SARS-CoV-2 Infection Boosts MX1 Antiviral Effector in COVID-19 Patients. *iScience* **2020**, *23*, 101585.
(35) Blanco-Melo, D.; Nilsson-Payant, B. E.; Liu, W.-C.; Uhl, S.; Hoagland, D.; Møller, R.; Jordan, T. X.; Oishi, K.; Panis, M.; Sachs, D.; Wang, T. T.; Schwartz, R. E.; Lim, J. K.; Albrecht, R. A.; tenOever, B. R. Imbalanced Host Response to SARS-CoV-2 Drives Development of COVID-19. *Cell* **2020**, *181*, 1036−1045.
(36) Lei, X.; Dong, X.; Ma, R.; Wang, W.; Xiao, X.; Tian, Z.; Wang, C.; Wang, Y.; Li, L.; Ren, L.; Guo, F.; Zhao, Z.; Zhou, Z.; Xiang, Z.; Wang, J. Activation and evasion of type I interferon responses by SARS-CoV-2. *Nat. Commun.* **2020**, *11*, 3810.
(37) Schroeder, S.; Pott, F.; Niemeyer, D.; Veith, T.; Richter, A.; Muth, D.; Goffinet, C.; Müller, M. A.; Drosten, C. Interferon antagonism by SARS-CoV-2: a functional study using reverse genetics. *Lancet Microbe* **2021**, *2*, e210−e218.
(38) Siu, K.-L.; Kok, K.-H.; Ng, M.-H. J.; Poon, V. K. M.; Yuen, K.-Y.; Zheng, B.-J.; Jin, D.-Y. Severe acute respiratory syndrome coronavirus M protein inhibits type I interferon production by impeding the formation of TRAF3.TANK.TBK1/IKKepsilon complex. *J. Biol. Chem.* **2009**, *284*, 16202−16209.
(39) Lui, P. Y.; Wong, L. Y.; Fung, C. L.; Siu, K. L.; Yeung, M. L.; Yuen, K. S.; Chan, C. P.; Woo, P. C.; Yuen, K. Y.; Jin, D. Y. Middle East respiratory syndrome coronavirus M protein suppresses type I interferon expression through the inhibition of TBK1-dependent phosphorylation of IRF3. *Emerg. Microb. Infect.* **2016**, *5*, No. e39.
(40) Zheng, Y.; Zhuang, M.-W.; Han, L.; Zhang, J.; Nan, M.-L.; Zhan, P.; Kang, D.; Liu, X.; Gao, C.; Wang, P.-H. Severe acute respiratory syndrome coronavirus 2 (SARS-CoV-2) membrane (M) protein inhibits type I and III interferon production by targeting RIG-I/MDA-5 signaling. *Signal Transduction Targeted Ther.* **2020**, *5*, 299.

https://doi.org/10.1021/acs.jproteome.1c00783
J. Proteome Res. XXXX, XXX, XXX−XXX